JOURNAL OF MATERIALS SCIENCE **34** (1999) 515–533

Processing, physical and thermal properties of Blackglas™ matrix composites reinforced with Nextel™ fabric

SRIRAM RANGARAJAN*, RONALD BELARDINELLI, PRANESH B. ASWATH†
Materials Science and Engineering Program, University of Texas @ Arlington, P.O. Box 19031, Arlington, TX 76019

The cure and pyrolysis behavior of a Blackglas™ resin and Nextel™ 440 impregnated with Blackglas™ resin were studied. Cure of the Blackglas™ resin is an exothermic process and DSC studies indicate that with an increase of catalyst content from 0.1 to 1.0%, the onset and peak temperature of cure are decreased coupled with an increase in the enthalpy of cure indicating a greater extent of cross linking. However, pyrolysis char yield of the pyrolyzate is relatively insensitive to cure conditions.

Cure pressure and pyrolysis environment are variables in the processing of Blackglas™ matrix composite reinforced with Nextel™ 440 plain weave fabric. Variations in cure pressure from 30 to 80 psi had no discernible effect on the chemistry of the pyrolyzate. However, the higher cure pressure resulted in top and bottom ply damage. Pyrolysis in an Ar environment resulted in incorporation of up to 12 wt % C of which 8 wt % was graphitic in nature in the ceramic matrix. Pyrolysis in NH_3 resulted in 3.9 wt % nitrogen and 1.5 wt % carbon in the matrix, with all the nitrogen and carbon bonded to Si. The cured panels have to be pyrolyzed/densified between 6–7 times to achieve required density and porosity content. Oxidation behavior of the composites at 1000 °C indicate that the argon pyrolyzed CMC's lose more weight due to decomposition of the pyrolytic carbon, whereas, NH_3 pyrolyzed CMC's are stable as both the N and C are bonded to Si in the matrix. Dielectric constants K′ and K″ measured at 1 GHz in the as-processed condition are high in the argon pyrolyzed CMC, ($K' = 11$–28) due to the presence of pyrolytic carbon. On the other hand NH_3 pyrolyzed CMC exhibit low dielectric constant ($K' = 4$). On oxidation, the dielectric constant in both the Ar and NH_3 pyrolyzed panels is approximately 4.0.

1. Introduction

The polymer pyrolysis route to processing of ceramics and ceramic matrix composites (CMCs) is being actively developed. Many different preceramic polymers have been discovered since their original development by Yajima *et al*. [1, 2]. These polymers on thermal treatment transform into a variety of ceramics, such as, SiC from polysilanes, Si_3N_4 from polysilazanes, Si–O–C silicon oxycarbides from polysiloxanes, silicon oxynitride, silicon carbonitride [3–7]. The interest in these materials has been spurred by their potential for low cost, ease and lower temperature of processing.

Recent work with polysiloxanes has attracted attention because they can be transformed into relatively high yielding (75–80% ceramic yield) Si–O–C ceramics when pyrolyzed in the 800–1000 °C range [6–9]. Pyrolysis beyond 1100 °C results in a carbothermal reduction into SiC, SiO_2, SiO(g) and CO(g). The simultaneous incorporation of carbon and oxygen in the matrix results in a metastable glassy phase with an increased resistance to devitrification [10], which is useful as a matrix in CMC's [11] in the intermediate temperature range (800–1100 °C).

In general, preceramic polymers contain a backbone chain of silicon or silicon and O/N with alkyl (e.g. $-CH_3$, $-C_2H_5$ etc.) or aryl (e.g. $-C_6H_5$) substituents attached to the silicon. In siloxane based precursors, the backbone is made up of Si–O units. These polymers are typically converted to ceramics in two stages. In stage one, the polymer is cured and crosslinked into a solid. In stage 2, the cured solid is pyrolyzed in an inert/reactive environment, where it is transformed into a ceramic with the simultaneous emission of gases such as hydrogen and hydrocarbons. This is schematically illustrated in Fig. 1a. Typically, silicon oxycarbide glasses (SiO_xC_y), have silicon in multiple

* *Present address*: Post Graduate Research Associate, Center for Ceramic Research, Rutgers University, Piscataway, NJ.
† Author to whom all correspondence should be addressed.

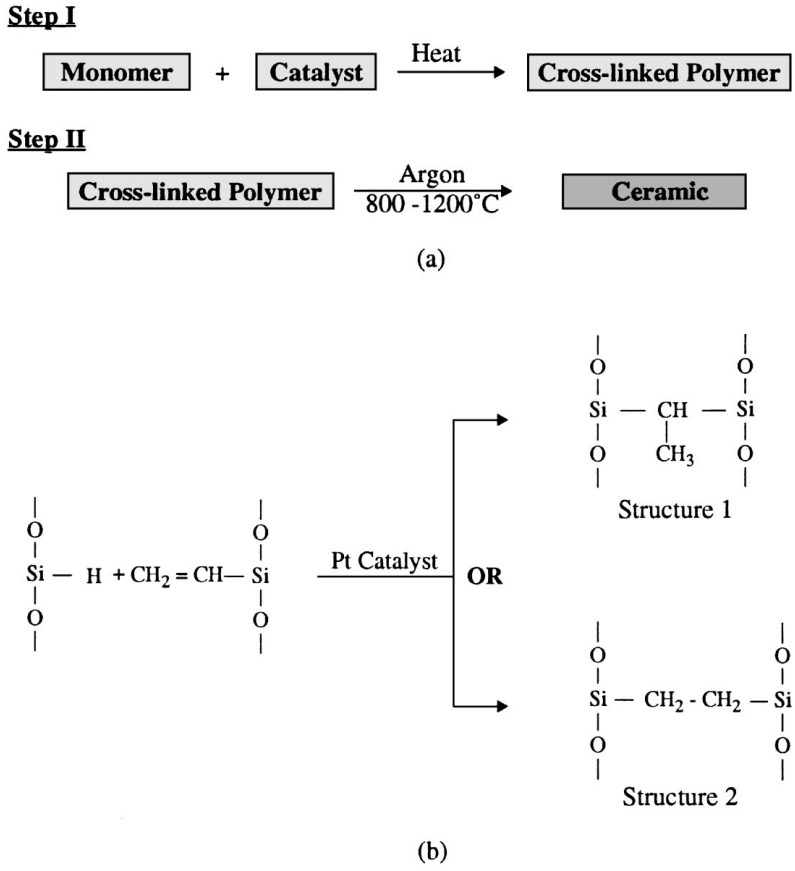

Figure 1 Schematic illustration of the polymer pyrolysis process.

configurations and carbon present in both the network structure and as free carbon. Many factors effect the structure and chemistry of the pyrolyzate. The degree of crosslinking and branching in the cured product [12], pyrolysis temperature and atmosphere [13] are known to have an effect on the pyrolyzate. However, the specific effect of these variables on the mechanism of transformation is not completely understood.

Polymeric precursors like polysilazanes have been used to synthesize high tensile strength ceramic fibers (Nicalon^{TM} SiC fibers). But precursors like polysiloxanes are ideal candidate matrices since they form a glassy ceramic on pyrolysis. The ceramic product has a lower associated shrinkage which reduces the residual stresses and cracking. However, other causes for an increased flaw structure exist. The evolution of gaseous products during pyrolysis results in porosity at both the micro and nano levels causing a degradation in the mechanical properties. This appearance of porosity requires additional infiltration, cure and pyrolysis cycles to reduce the porosity levels in the composite and build up the thermomechanical properties.

The objective of this study was to determine the effect of cure and pyrolysis variables on the structure and composition of the ceramic product. The preceramic polymer studied was an Allied Signal proprietary material called Blackglas^{TM} (solution 489A). In addition, CMCs using Blackglas as matrix were processed under differing conditions to assess the effect of processing variables on the structure, composition and properties of the CMCs. The variables studied were cure pressure and pyrolysis atmosphere.

2. Experimental

This section is divided into three sub-sections. In the first section, the experiments performed on the pure Blackglas resin 489A are reported. In the second section, the processing of ceramic matrix composites with Blackglas resin and Nextel^{TM} 440 fibers is discussed. Finally, the methods of characterization of the physical, oxidation and electrical properties are presented.

2.1. Cure and pyrolysis of Blackglas resin

Blackglas resin 489A was used with 489B as the catalyst in all the experiments with the matrix materials. Differential Scanning Calorimetry (DSC) studies were performed on samples of Blackglas resin using a Perkin Elmer Series 7000 DSC thermal analyzer system. Samples with three different catalyst contents of 0.1%, 0.5% and 1.0%, were studied from 25 °C through 200 °C at a heating rate of 5 °C/min. The enthalpy of cure, the reaction start temperature, the peak temperature and the finish temperature were evaluated from these experiments.

In order to study the mechanism of pyrolysis of Blackglas resin, samples were first cured in air at 75 °C and 150 °C with different amounts of catalyst for 180 min. The cured polymer samples with 0.1, 0.5 and 1.0% catalyst ratios were then pyrolyzed into silicon oxycarbide ceramics by heating to 982 °C under an inert Ar atmosphere. The gravimetric analysis of the pyrolysis was performed using two different procedures. Small samples (~ 100 mg) were pyrolyzed in a Seiko Thermo Gravimetric Analyzer (TGA) by heating from 25 to

1000 °C at 10 °C/min. Bigger samples (∼ 1 g) were pyrolyzed in tube furnace from 25 to 982 °C at 5 °C/min. In both cases high purity argon (99.99%) at a 100 cc/min flow rate was used.

Chemical analysis was performed on the pyrolyzed samples by Quantitative Technologies Inc. New Jersey, to determine the effect of curing condition on the chemistry of the pyrolyzate. The C, H and N analysis was performed using optimum combustion techniques. The Si analysis was performed using Atomic Absorption Spectroscopy after digestion of the sample. Oxygen analysis was not performed.

In order to study the types of chemical bonds present after the cure and pyrolysis process infra red (IR) spectroscopy was performed using a Biorad FTIR. Cured and pyrolyzed samples were powdered and mixed with KBr to obtain the spectrum in the diffuse reflectance mode. X-ray photoelectron spectroscopy (XPS) analysis was performed using an Perkin Elmer PHI 5000C on powdered pyrolyzed samples using an AlK_{α} wavelength. The charge effect was compensated using a neutralizer gun. High resolution scans of Si_{2p}, O_{1s} and C_{1s} peaks were obtained to determine the chemical bond configurations of the pyrolyzate.

2.2. Processing of the Blackglas matrix composite

3M Nextel™ 440 BF18 plain weave fabric was prepregged with Blackglas resin 489C (a more viscous version of 489A) by Allied Signal Inc., Des Plaines IL. Prior to prepregging, the fabric was coated with a 0.1 μm thick pyrolytic carbon by Synterials Inc., Herndon, VA. using a chemical vapor deposition (CVD) technique. The final prepreg composition was 46.7 wt % resin and 53.3 wt % fiber. The prepreg was subjected to the processing sequence shown in Fig. 2.

The layup procedure used was the following. The prepreg was removed from the freezer and allowed to equilibrate to room temperature. 15 cm × 15 cm plies were cut using an aluminum template. Stacking of plies into 6 or 12 ply laminate panels in the sequence 0/90 was made with the warp dominant surface down, followed by matching of warp and fill predominant surfaces. After stacking, all panels were weighed, bagged and debulked. Following debulking, a thermocouple was placed into the panels and the vacuum bag was installed. Fig. 3 shows a schematic of the layup. The panels were then autoclave cured using the cure cycle presented in Fig. 4a. As can be seen from Fig. 4a, the panels were exposed to a maximum temperature of 150 °C following a hold at 65 °C. A 30 or 80 psi autoclave compaction pressure was applied during the curing cycle. After cure, the panels were visually inspected, followed by ultrasonic and X-ray NDE and finally trimmed.

The cured panels were then placed in a furnace retort and pyrolyzed in either argon or ammonia atmosphere. The panels were heated up to 871 °C using a pyrolysis cycle shown in Fig. 4b. Pyrolysis gas flow rate through the retort was 60 cc/s. Pyrolysis results in a significant weight loss in the matrix along with an increase in porosity. Panels were then subjected to further processing (densification cycles, Fig. 4c) by reinfiltration of the panels with Blackglas resin 489A, followed by curing and re-pyrolysis. Densification of the panels was achieved using a pressure/vacuum apparatus. The panel was laced into the unit and first evacuated, followed by

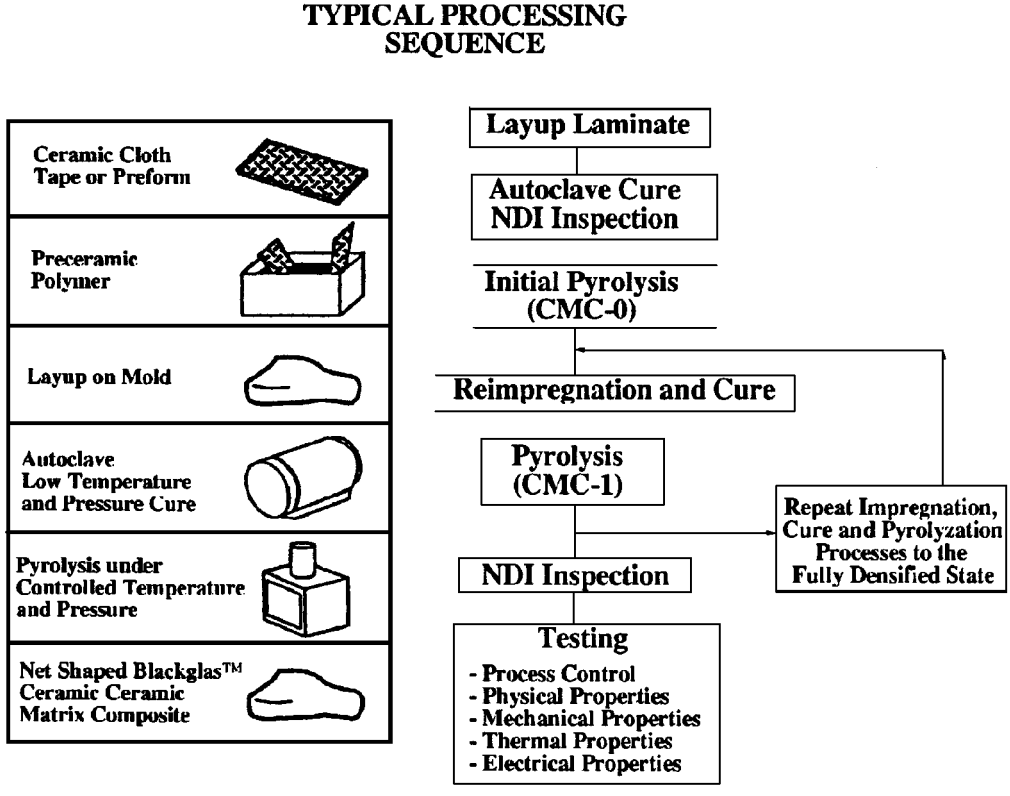

Figure 2 Flow chart of the experimental method used in processing Blackglas matrix composites.

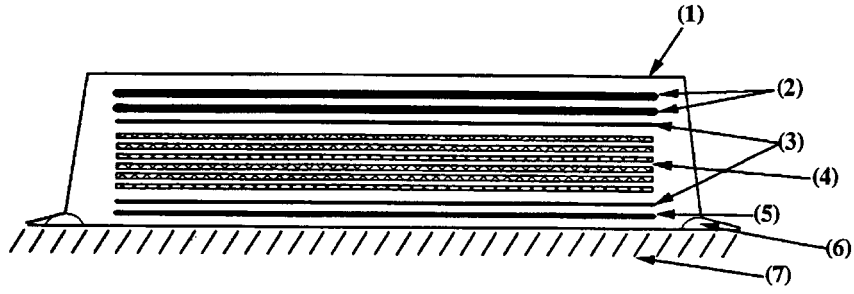

(1) Nylon Bagging Film
(2) Vent Cloth
(3) Peel Ply
(4) Blackglas Laminate: 6 or 12 plies of Prepreg
(5) Teflon Film
(6) Bag Sealing Compound
(7) Aluminum Layup Plate

Figure 3 Schematic showing the layup of the composite panel prior to its introduction into the autoclave for the cure cycle.

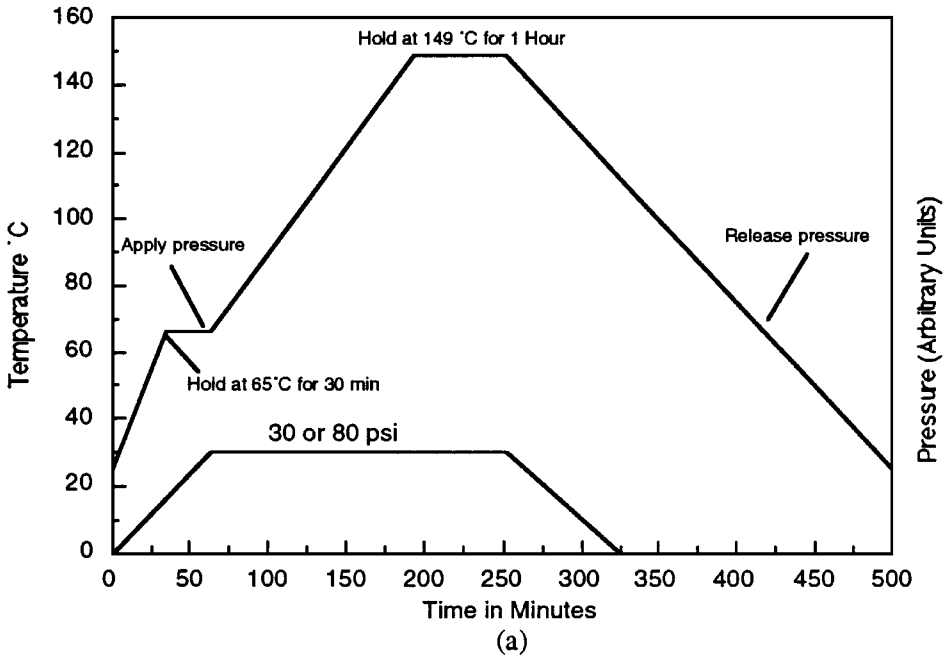

(a)

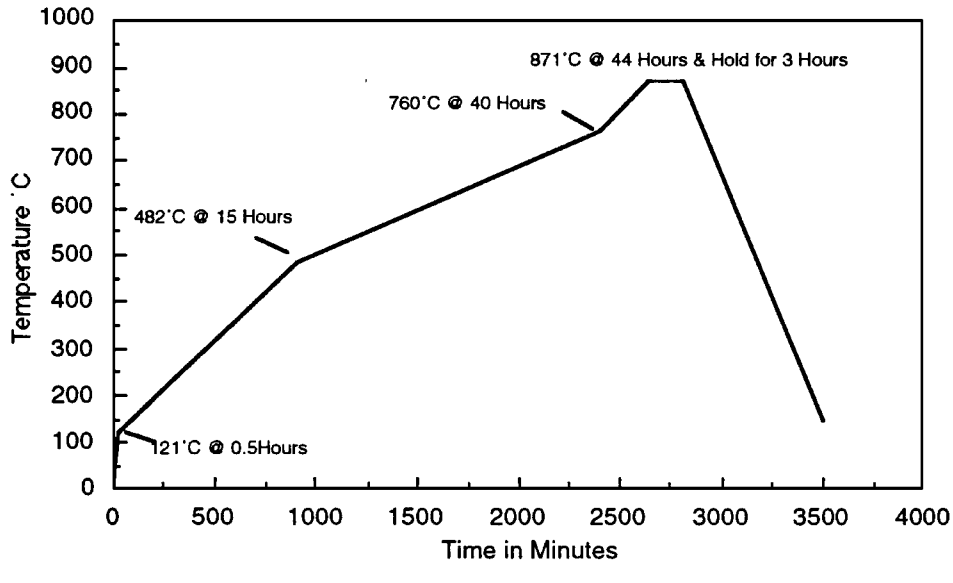

(b)

Figure 4 The time-temperature cycles used for the processing of the composites: (a) the autoclave cure cycle, (b) the pyrolysis cycle and (c) the densification cycle. (*Continued*).

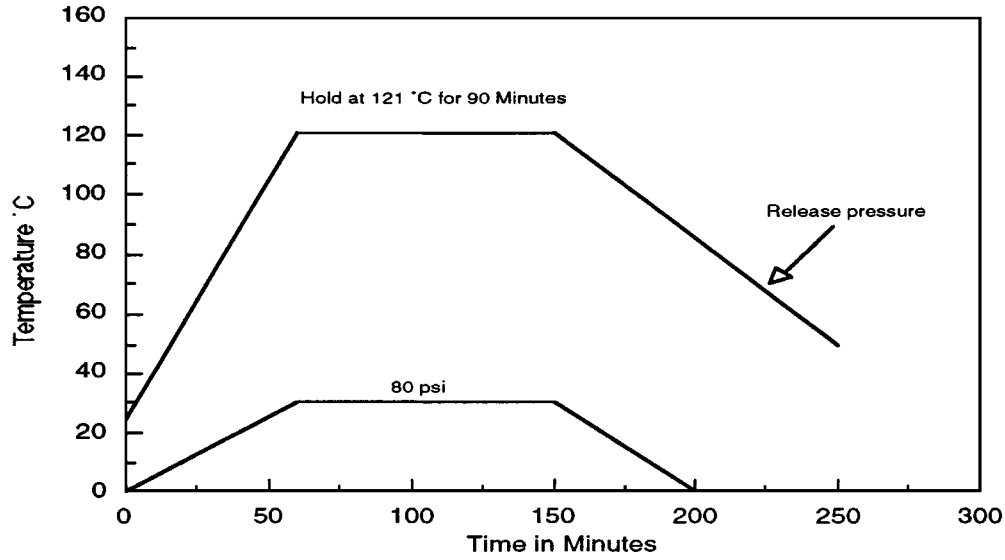

(c)

Figure 4 (*Continued*).

TABLE I Table giving the panel identification and processing condition for all. Also shown is the key processing variable studied for each panel

Panel name	Cure pressure	Pyrolyzing atmosphere	Comment
P30	30 psi	Argon	Baseline
P80	80 psi	Argon	Effect of autoclave cure pressure
PNH_3	30 psi	NH_3	Effect of pyrolysis environment

the introduction of the resin Blackglas 489A mixed with catalyst into the panel. Following the vacuum impregnation, the panels were subjected to a 80 psi pressure to force the resin into all the pores. The impregnated panels were then cured and pyrolyzed. More than one densification cycle was required and this process of re-infiltration, curing and pyrolysis was continued until relative weight gain in ceramic matrix over the previous step was < 1%. It was found that 5–6 densification/pyrolysis cycles were required to reach a point of diminishing returns, after which subsequent densification and pyrolysis did not result in more than 1% weight gain.

The panels were subjected to process control tests i.e., pyrolysis weight loss, dimensional, volume and porosity measurements at each processing step. Following final pyrolysis, the panels were again examined for flaws using visual and NDE inspection techniques. Six panels were processed and two processing variables were studied. The processing variables included the effect of autoclave cure pressure and the effect of pyrolysis atmosphere on the composite properties. Panel nomenclature along with the processing conditions and variables is summarized in Table I.

2.3. Characterization of the physical, electrical and oxidation properties of Blackglas matrix composites

The Blackglas CMCs were subjected to the following characterization and analysis procedures. Open porosity was measured using a modified ASTM C-20 method [14]. Here, instead of infiltration with boiling water, the panels were pressure/vacuum infiltrated before measuring wet weight. Chemical analysis similar to the method used in the analysis of Blackglas ceramic was performed on the composites to determine the chemical composition. Optical and scanning electron microscopy was performed on samples cut from the three panels, to observe the cross section microstructure. The cross-section samples were cut, cold mounted and gradually polished so as to minimize cracking during the process.

Oxidation behavior of the C-coated Nextel 440 fabric was performed on a Seiko TGA by heating up from room temperature to 1050 °C at a rate of 10 °C/min in an environment of flowing air at 100 cc/min. Oxidation behavior of the pyrolyzed panels were examined using samples 25 × 25 mm in dimension in a tube furnace in a static air environment. Thermomechanical analysis (TMA) was performed in the temperature range of 25–1150 °C using a heat up rate of 10 °C/min in an environment of flowing air 200 cc/min in a Seiko TMA on the pyrolyzed panels both in the in-plane and out-of-plane orientation using two samples for each case. Samples of the composite were used to evaluate the effects of processing variables on the electrical properties. The permittivity at X-band (8–12 GHz) was measured on waveguide specimens 25 × 25 mm in dimension in the as-processed state and after oxidation at 815 and 982 °C for up to 100 h using an Hewlett Packard 8510B Network Analyzer.

3. Results and discussion

3.1. Cure and pyrolysis of Blackglas resin

3.1.1. The hydrosilyation reaction

The process by which a silicon-carbon bond is synthesized by addition of organosilanes/siloxanes that contain silicon hydrogen groups to organic compounds with terminal double bonds is called a hydrosilyation

reaction [15–17]. In the cure of Blackglas resin, a simplified representation of the cure reaction where A and B are two functional groups in the monomer is given by

$$\sim A + B\sim + \text{ Catalyst} \rightarrow \sim AB\sim + \text{ Catalyst} \quad (1)$$

This type of reaction is typical of step polymerization in which the catalyst is regenerated after the completion of the reaction, is also representative of the hydrosilylation reaction. Neglecting the effects of multifunctionality (> 2) of the monomer units and assuming equal reactivity of the functional groups,

$$\text{Rate of reaction} = -\frac{\text{d[A]}}{\text{d}t} = \frac{-\text{d[B]}}{\text{d}t} = K[\text{A}][\text{B}][\text{Catalyst}] \quad (2)$$

where $K = \text{Rate constant} = K_0 \cdot \exp(-\Delta H/RT)$, K_0 is the temperature independent constant, ΔH is enthalpy of reaction, T is temperature and R is gas constant. So the curing kinetics is affected not only by time and temperature of curing, but also the catalyst concentration. For this study, one or more cyclosiloxane monomer(s) having the general formula,

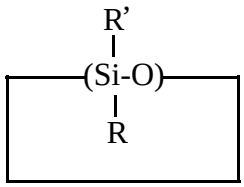

were used as the starting material [5]. In this monomer, n is an integer between 3 and 30, R and R′ are a combination of hydrogen, alkene (C_nH_{2n} hydrocarbons) and alkyl (–CH_3, –C_2H_5 etc.) groups. In these alkene and alkyl groups at least one vinyl carbon atom is directly bonded to Si [5]. The chemistry of the monomer is proprietary to Allied Signal Corporation. The catalyst used in the reaction are complexes of platinum which yield very few by products. The exact chemical nature of the catalyst and Blackglas resin 489B is proprietary to Allied Signal Corporation, Morristown, NJ.

The results of the tests performed on the Blackglas 489A solutions containing 0.1%, 0.5% and 1.0% catalyst to study the curing characteristics is outlined below.

3.1.2. Effect of catalyst concentration on the curing of Blackglas resin

The hydrosilylation reaction between H and vinyl groups (–CH=CH_2) attached to Si atoms is typically catalyzed by platinum [15]. This reaction is schematically represented in Fig. 1b. Blackglas, which is made up of siloxane backbone with H and vinyl groups attached to silicon, has a functionality (of the monomer units) greater than 2.

In case of the multifunctionality of the monomer units, polymerization leads to network formation and cross-linking. Typically, such polymers exhibit a gel point at which point the reaction medium achieves sufficient viscosity and restrains the mobility of the catalyst molecules to active sites. Fig. 5 shows the effect of catalyst concentration on the enthalpy of the curing reactions. Table II details the reaction start and peak temperature along with the heat of reaction. The heat of reaction is corrected for weight loss due to vaporization of the low molecular weight monomer units. Since curing of Blackglas is an addition polymerization reaction, there are no by-products to the reaction. Weight loss in the curing process is due only to evaporation of the monomer. To confirm this, a DSC experiments were performed on the pure Blackglas solution (0% catalyst). Although the weight loss in this case was $\sim 75\%$, no reaction peaks were observed. From the Table II it is clear that the heat of reaction is exothermic and is a function of the catalyst concentration. With an increase in the catalyst content, the ΔH increases and T_{onset} and T_{peak} temperatures decrease. The T_{peak}, which is a measure of the reaction rate, decreases as ΔH increases, in accordance with Equation 2. Therefore faster kinetics and a larger number of active sites at higher concentration of catalyst cause a greater extent of curing yielding a larger heat of reaction.

TABLE II Summary of the effect of catalyst content on the DSC results on Blackglas resin

% Catalyst	Onset (°C)	Peak (°C)	ΔH_{corr} (J/g)
0.1%	104.7	137.5	−244.6
0.5%	68.4	106.7	−370.7
1.0%	65.8	102.6	−430.5

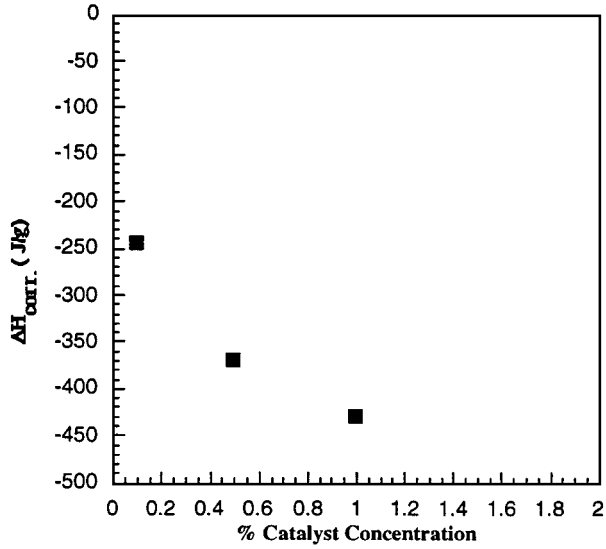

Figure 5 The effect of amount of catalyst mixed with Blackglas precursor 489A on the heat of reaction obtained from DSC experiments.

3.1.3. Effect of temperature and time on the curing of Blackglas resin

DSC test runs in conjunction with IR spectroscopic techniques were used to determine the effect of temperature and time of cure on the characteristics of the Blackglas 489A resin mixed with different amounts of catalyst. Samples cured at varying temperatures and

TABLE III Test matrix of cure and DSC experiments on Blackglas resin solution

% Catalyst	Cure temp. (°C)	Cure time (min)	DSC
0.1%	75	180	√
0.1%	150	180	×
0.5%	75	180	√
0.5%	150	180	√
1.0%	75	180	×
1.0%	150	180	×

times were subsequently analyzed using DSC and IR spectroscopy. The test conditions are summarized in Table III. Samples containing 0.1%, 0.5% and 1.0% catalyst content were cured at 75 and 150 °C for 180 min. Neither the cure temperature nor the catalyst content had any significant differences on the characteristics of the IR spectrum. Fig. 6 is a representative IR spectra of the Blackglas 489A solution with 0.5% catalyst cured at 150 °C for 180 min. Since the IR spectra of the Blackglas solution could not be obtained due to proprietary restrictions, the actual polymerization mechanism and the extent of curing can only be qualitatively assessed by comparing the spectra of the cured samples. Curing was studied by monitoring the peaks attributed to Si–H (2154 cm^{-1}) and Si–vinyl (1597 cm^{-1}) [18] groups. Differences in the peak height among the different cure conditions indicate that with increase in temperature of cure and catalyst content, the intensity of the Si–H and C=C (Si–vinyl) stretch decreases suggesting a greater extent of cure. From Tables IV and Fig. 7 it can be seen that the kinetics of curing of 0.1% sample at 75 °C is slow and complete cure is not achieved even after 180 min. Hence DSC run on the post 75 °C cured samples of Blackglas show an exotherm due to post curing. But on increasing either the catalyst content or the cure temperature, the exotherm disappears.

Additional studies were conducted to examine the cure kinetics at a fixed catalyst content and cure

TABLE IV DSC test results showing effects of catalyst content, cure time and temperature on the onset temperature, peak temperature and enthalpy of post cure

% Catalyst	Cure temp (°C)	Cure time (min)	Post cure characteristics		
			Onset (°C)	Peak (°C)	ΔH_{corr} (J/g)
0.1%	75	180	124.4	147.7	−7.6
0.5%	75	180	—	—	0
0.5%	NA[a]	0	68.4	106.7	−370.7
0.5%	150	2	No peak	No Peak	−0.8
0.5%	150	180	No Peak	No Peak	0

[a]NA = Not applicable.

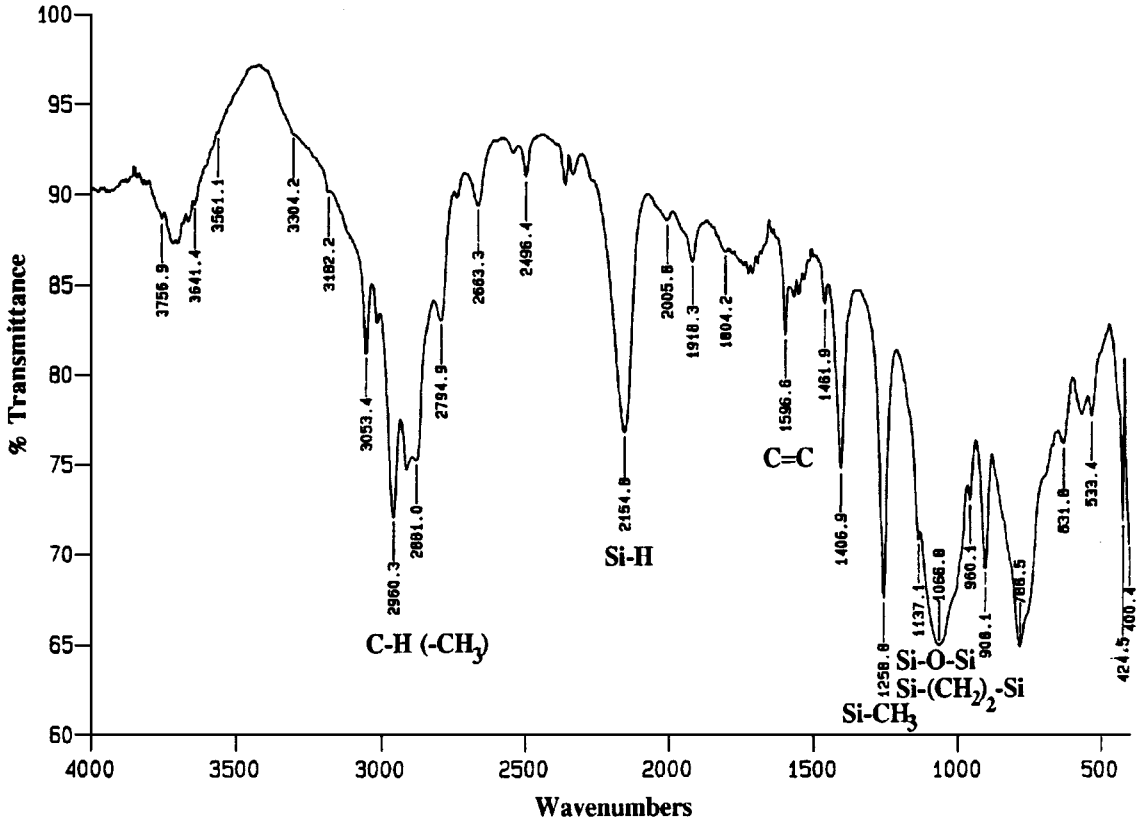

Figure 6 Representative IR spectra of cured sample of Blackglas resin mixed with catalyst and cured. This particular sample was mixed with 0.5% catalyst and cured at 150 °C for 180 min.

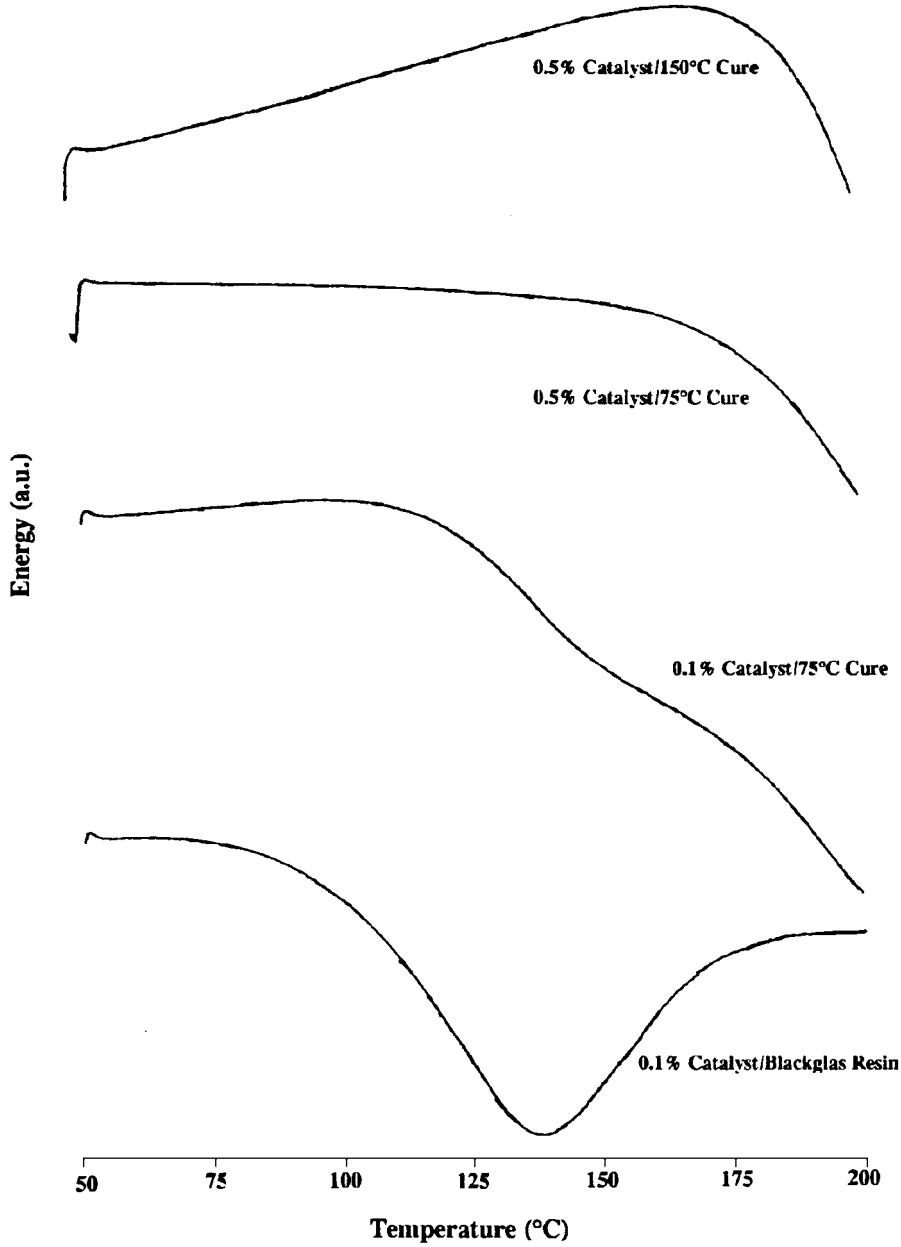

Figure 7 DSC runs of cured Blackglas resin mixed with different amounts of catalyst and cured at different temperatures. The cure conditions were 0.1%/75 °C, 0.5%/150 °C and 0.5%/75 °C, with all samples cured for 180 minutes at temperature. The DSC runs indicate incomplete curing in the 0.1%/75 °C Blackglas sample.

temperature. Blackglas resin with 0.5% catalyst were cured at 150 °C for different time intervals were then reheated on the DSC. Fig. 8 shows the plot of ΔH vs. time of curing. The cure kinetics for this reaction as can be seen from the plot is very fast. Expressing the extent of reaction as $\Delta H_{(\text{post cured Blackglas})}/\Delta H_{(\text{Blackglas resin})}$, it can be seen that even a short time of 2 min is enough to complete 99% of the reaction.

3.1.4. Pyrolysis of the cured Blackglas product

Table V details the pyrolysis yield (wt. of ceramic/wt. of cured polymer) of the Blackglas ceramics obtained through pyrolysis of samples cured under different conditions. It is evident that the curing conditions did not change the pyrolysis yields much. This is surprising, since extent of cross-linking has been shown to have a

TABLE V Pyrolysis yields and carbon content of ceramic as a function of catalyst content and cure temperature. All samples were cured for 180 min

% Catalyst	% Yield			% Carbon	
	75 °C	100 °C	150 °C	75 °C	150 °C
0.1	81.6	NAF	82.4	22.3	25.7
0.5	82.4	82.3	82.5	28.1	26.9
1.0	82.0	NAF	83.0	NAF	NAF
0.5 + 70 psi	NAF	82.9	NAF	NAF	NAF

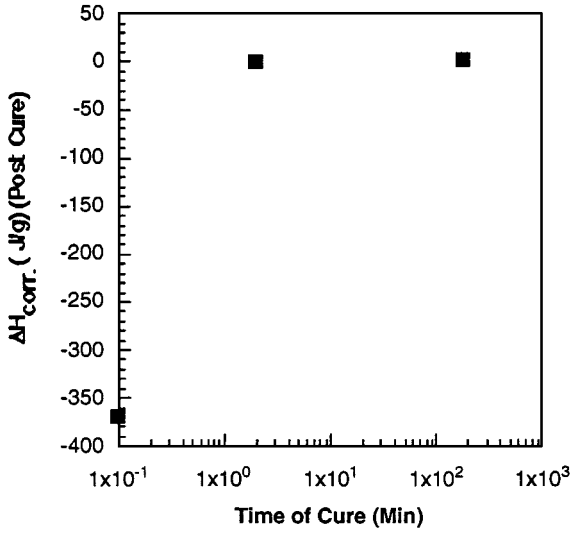

Figure 8 Curing kinetics of Blackglas solution 489A containing 0.5% catalyst cured for different times at 150 °C.

strong effect on the pyrolysis yields [12]. In order to explain this apparent anomaly, the samples were further analyzed for chemical composition and using IR and XPS spectroscopy. Fig. 9 shows the IR spectrum of the argon pyrolyzed samples. Comparing Figs. 6 and 9, most peaks present in the precursor disappear on pyrolysis and are replaced by a broad peaks of Si–O–Si and Si–C stretches at 1065 cm^{-1} and 810 cm^{-1}, respectively. The broad peak centered at 1837 cm^{-1} is attributed to amorphous carbon. CHN chemical analysis determined that the carbon content of the ceramics shows no particular trends except for one case. The Blackglas resin with 0.1% resin and cured at 75 °C had a lower carbon content (see Table VI) compared to the other samples. The reason for this may be attributed to the incomplete curing of this sample resulting in slightly lower yield and carbon content. XPS of the pyrolyzed Blackglas ceramic also did not reveal major differences in the characteristics of the bonding based on differences in the catalyst content or cure temperature. Fig. 10 is a representative spectra of the Blackglas matrix pyrolyzed in Ar at 982 °C, showing deconvoluted Si, C and O peaks. Both Si and C atoms show two major bond configurations. For Si atoms this arises because Si is bonded to both O and C atoms. Carbon on the other hand shows peaks matching C–C (graphitic) bonds at 284.3 eV and Si–C bond at 283.1 eV.

TABLE VI Table showing the chemistry, fiber volume fraction and porosity in the as processed Blackglas matrix composites as well as some basic information about monolithic Blackglas and Nextel 440 fibers

	Chemical composition							Fiber volume fraction (V_f)	Apparent porosity (%)
Panel ID	%Si	%O	%C	%H	%N	%Al	%B		
Matrix	40.57	NAF[a]	26.87	0.4	NAF	NAF	NAF	NA	5.0
Fiber	13.07	49.71	NAF	NAF	NAF	37.0	0.2	NA	NA
P30	NAF	NAF	11.65	0.13	NAF	15.0	< 0.1	31.57	3.29
P80	NAF	NAF	12.26	0.16	NAF	15.55	< 0.1	29.49	3.27
PNH_3	NAF	NAF	1.48	< 0.1	3.92	15.08	< 0.1	28.1	4.42

[a]NAF: Not analyzed for.

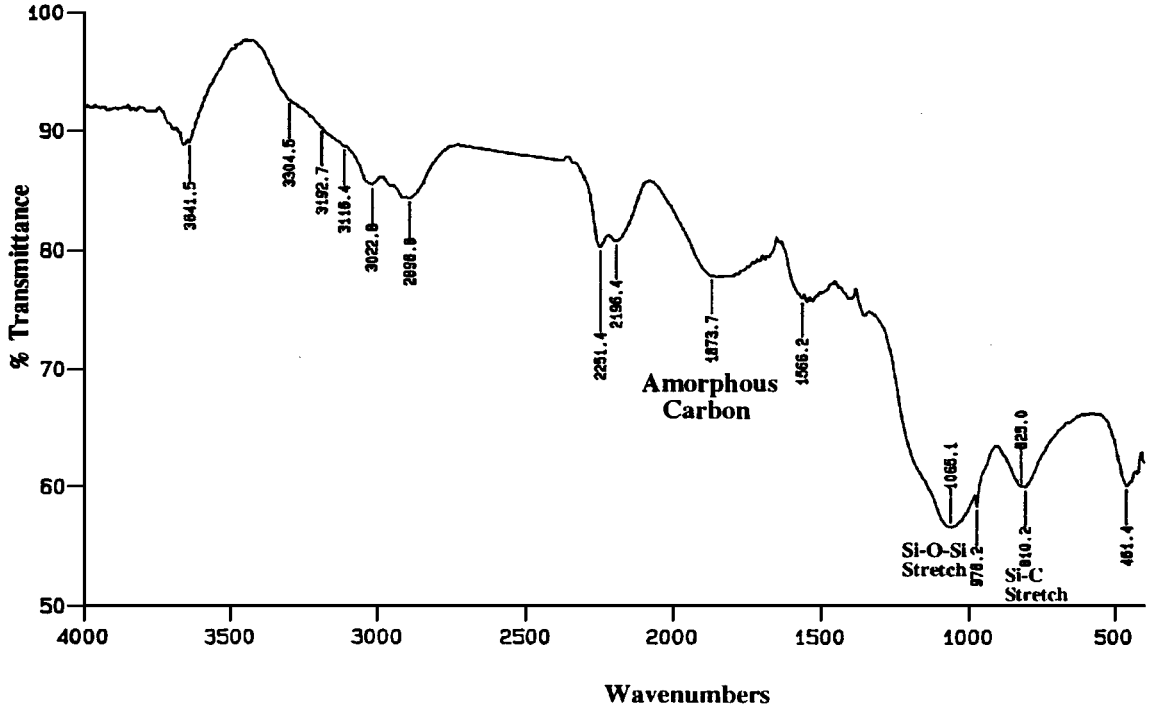

Figure 9 Representative IR spectra of the Blackglas ceramic pyrolyzed at 982 °C in an argon environment. This spectra corresponds to Blackglas resin with 0.5% catalyst cured at 150 °C.

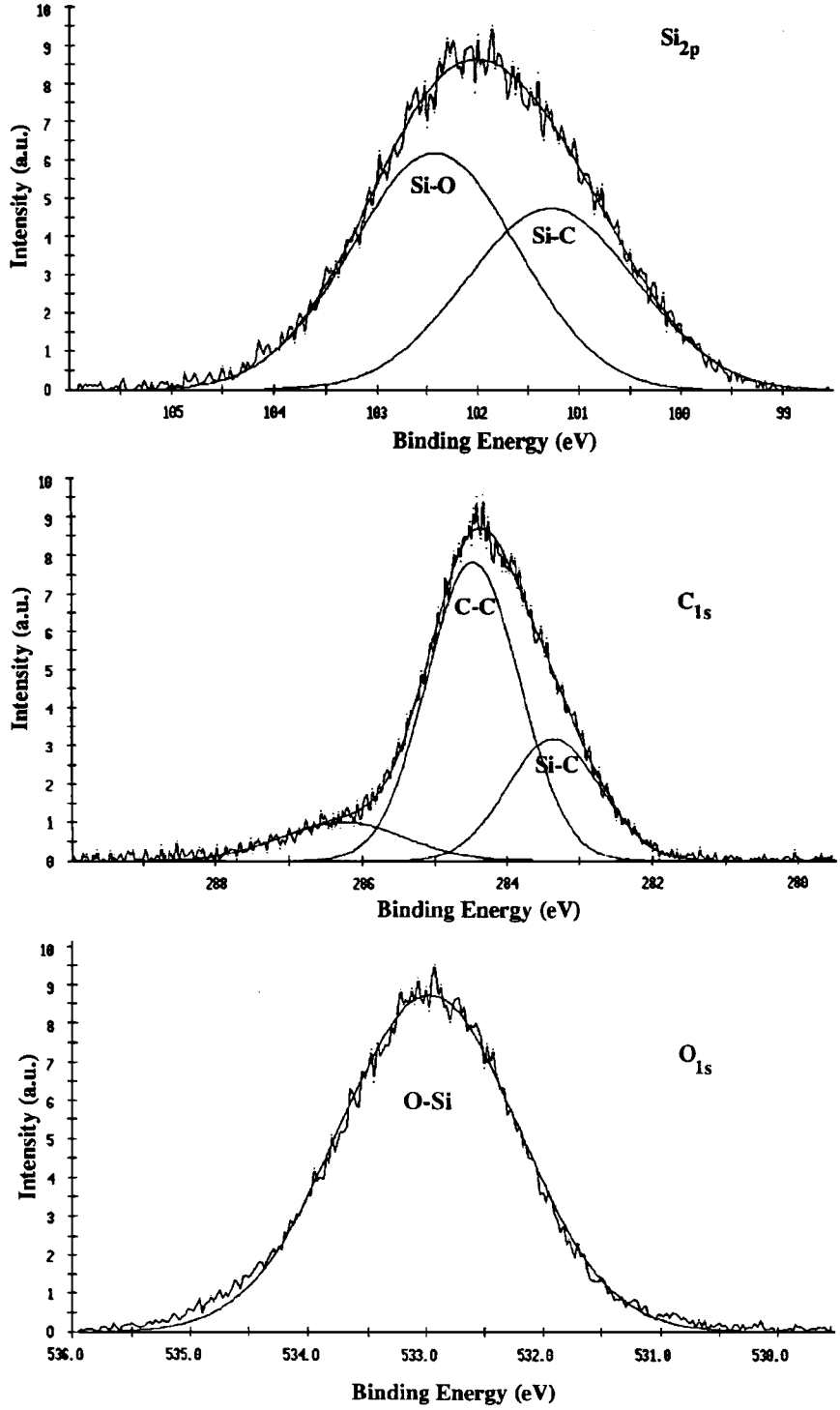

Figure 10 Representative XPS spectra of cured and pyrolyzed Blackglas ceramic. This particular XPS spectra is of a Blackglas resin 489A mixed with 0.1% catalyst cured at 150 °C for 180 min and subsequently pyrolyzed at 982 °C in Ar.

Two possible explanations for the minimal influence of catalyst content and cure temperature on the pyrolyzate are proposed. (i) It is clear that the curing conditions do not strongly affect the chemical composition, pyrolysis yield or the chemical structure of the pyrolyzates. This implies that either there is a threshold level beyond which cross-linking does not increase yield or that there is the possibility that the samples underwent complete curing during the initial stages of the pyrolysis process due to thermal activation. (ii) Lower yield and carbon content in product which had a 0.1% catalyst content and cured at 75 °C was possibly caused by the incomplete cure. Incomplete cure results in a higher degree of unreacted functional groups. During the initial stages of pyrolysis ($T < 300$ °C), the wt. loss (see Fig. 11) is probably associated with evaporation of volatile monomer units.

3.2. Implications of the cure and pyrolysis study for processing of Blackglas matrix composites

It has been determined that the kinetics of the hydrosilylation reaction is extremely fast and the controlling

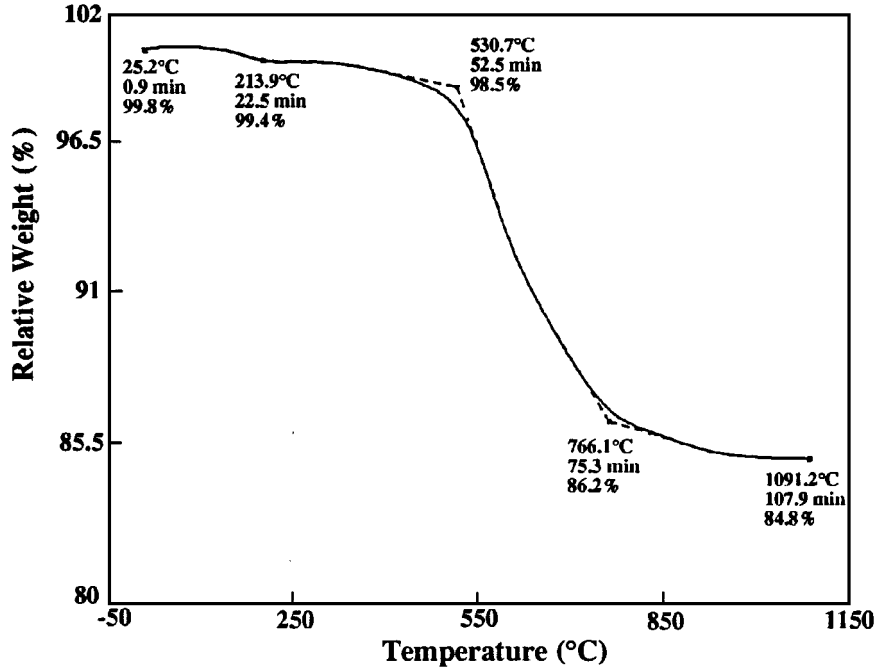

Figure 11 Thermogravimetric analysis of blackglas sample when heated from room temperature to 1100 °C under flowing argon.

factor in the cure process is the migration of catalyst to reaction site. The extent of curing is promoted by increasing the catalyst content and by increasing the temperature of cure. However, while processing composites, in particular, large parts and panels, slow and uniform curing is required to prevent delamination. Based on the results of the catalyst content and cure time/temperature on the characteristics of the structure and chemistry of the pyrolyzate, the cure cycle shown in Fig. 4a was adopted for processing of the composites. The cure cycle had a two step heating up to 150 °C with a 30 min hold at 65 °C to equilibrate. Two different cure pressures of 30 or 80 psi were used.

Fig. 11 a plot of weight change as a function of temperature derived from a thermogravimetric analyzer (TGA) of a representative cured Blackglas resin sample heated in a flow of Ar from room temperature to 1100 °C. Three distinctive regions can be identified. They are

Region I	$25- \approx 530\,^{\circ}C$
Region II	$530 - 766\,^{\circ}C$
Region III	$766 - 1100\,^{\circ}C$

Maximum weight loss ($\sim$ 12%) occurs in region II. This temperature range corresponds to the pyrolysis stage in which the pyrolyzate goes through a high surface area, high porosity and low density phase. In processing the Blackglas matrix composites a very slow heating rate was adopted in this temperature range to minimize the effects of shrinkage and porosity. Fig. 4b shows details of the pyrolysis schedule employed in the processing of the Blackglas matrix composites. In order to eliminate the porosity formed after the initial pyrolysis cycle (CMC-0) additional infiltration and cure cycle was performed as shown in Fig. 4c. Following this densification cycle, the normal pyrolysis cycle was repeated. This densification and pyrolysis cycles were repeated (CMC-1 and higher) till required decrease in the porosity content was achieved. The overall process cycle is represented in Fig. 1.

3.3. Processing of the Blackglas matrix composites

3.3.1. Process data

Process data such as density, porosity and weight loss on pyrolysis were monitored at each stage of the processing of the composites. Fig. 12a–c are the results of process data plotted as a function of the process step. The first pyrolysis cycle going from the cured state to CMC-0 is the most important step since this determines not only the number of subsequent infiltration/densification and pyrolysis steps to follow but also the microstructure and properties of the final composite. Pyrolysis of cured Blackglas resin results in porosity and shrinkage. Therefore on the first pyrolysis, density of the composite decreases, the porosity increases from 0% in the cured state to greater than 30% after CMC-0 accompanied by a weight loss of $>$ 5%. From Table VI it can be seen that the porosity in pure Blackglas matrix is approximately 5% which is much lower than that measured for the composites. The reason for this dissimilarity between the monolithic Blackglas and in the composite is that in the latter case the constraint and dissimilar shrinkage between matrix and fibers in the composite causes matrix cracking which contributes to the additional porosity in the composite. Fortunately, much of the porosity present after CMC-0 is interconnected and get filled up with resin on subsequent infiltration with Blackglas resin 489A during the densification process. On subsequent pyrolysis, (CMC-1 and higher), the porosity gradually

fills up with the pyrolyzed product and there is a steady increase in the density and decrease in open porosity of the composite as shown in Fig. 12a–c.

It can also be seen from the figures that the panels P30 and P80 behaved almost identically while the PNH_3 panel had greater weight loss and associated porosity at

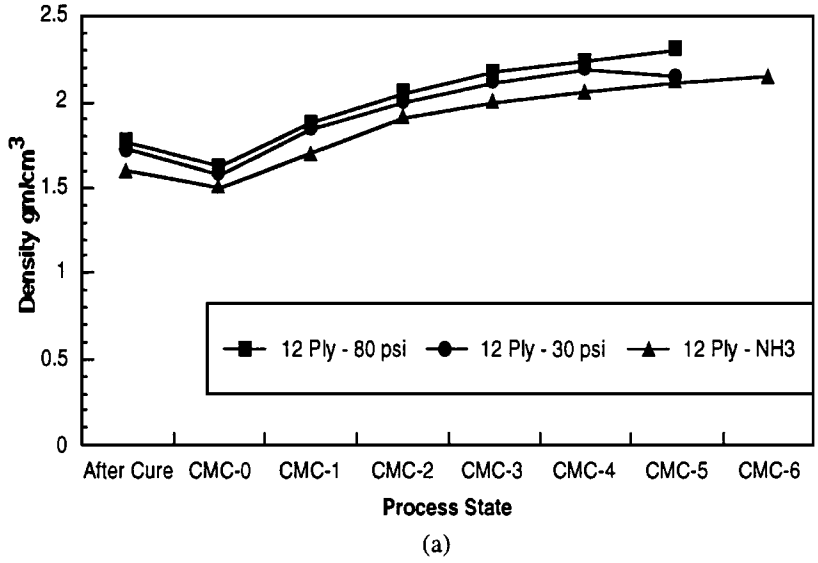

(a)

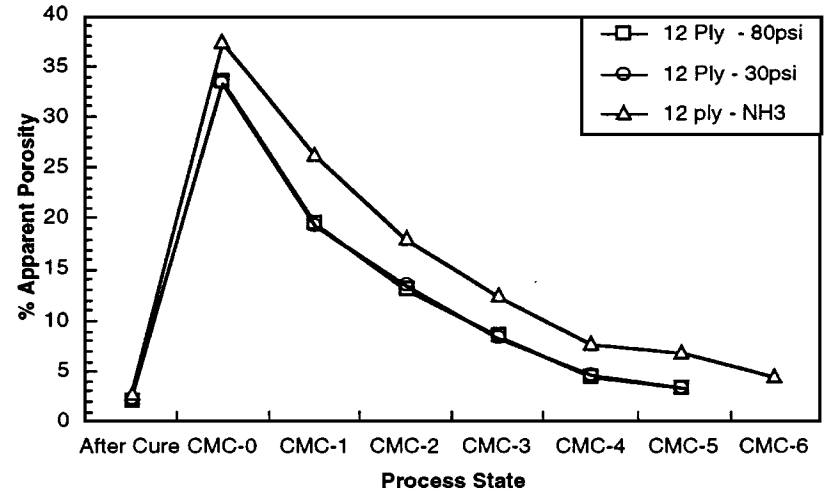

(b)

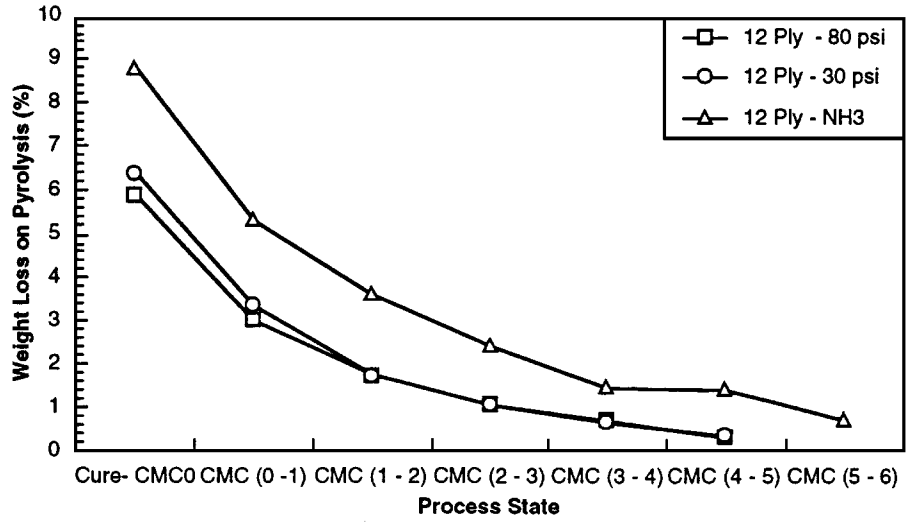

(c)

Figure 12 Process control variables as a function of the number of densification/pyrolysis cycles: (a) the density of the blackglas matrix composite, (b) porosity content and (c) weight loss after each densification/pyrolysis cycle.

each step. Therefore PNH_3 panels had to be processed one additional step (CMC-6) to achieve the same porosity levels as P30 and P80.

3.3.2. Pyrolyzed products

Two panels of each of the three experimental conditions were processed. The chemical composition of the panels, apparent porosity and the calculated fiber volume fraction of the composites are listed in Table VI. Also shown in the table, are the compositions of the original fiber and monolithic Blackglas processed through CMC-0 in an environment of Ar under similar conditions as the composite panels for comparison purposes. The chemical analysis data shows that panels P30 and P80 had a chemically different matrix in comparison

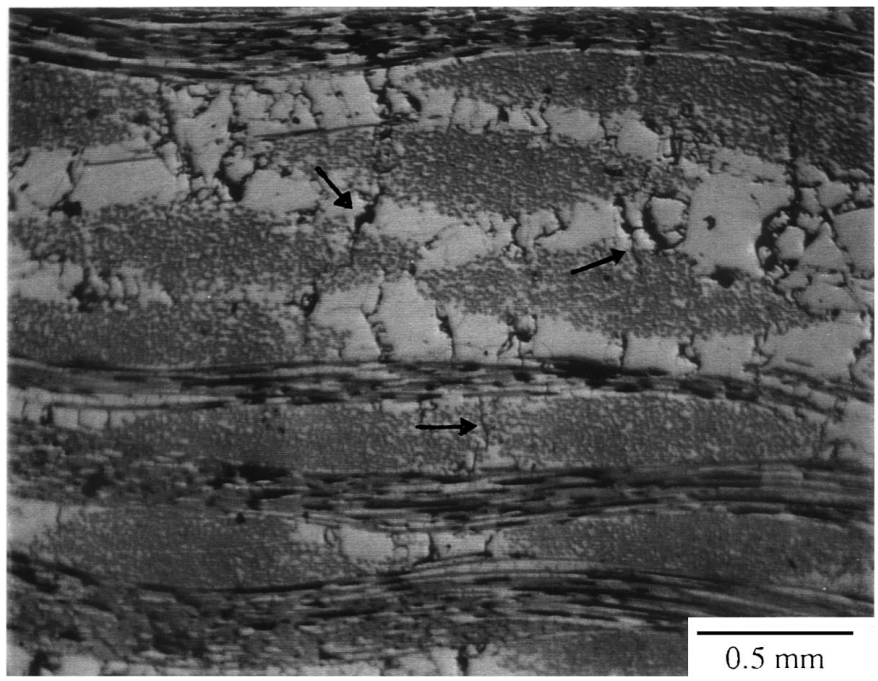

(a)

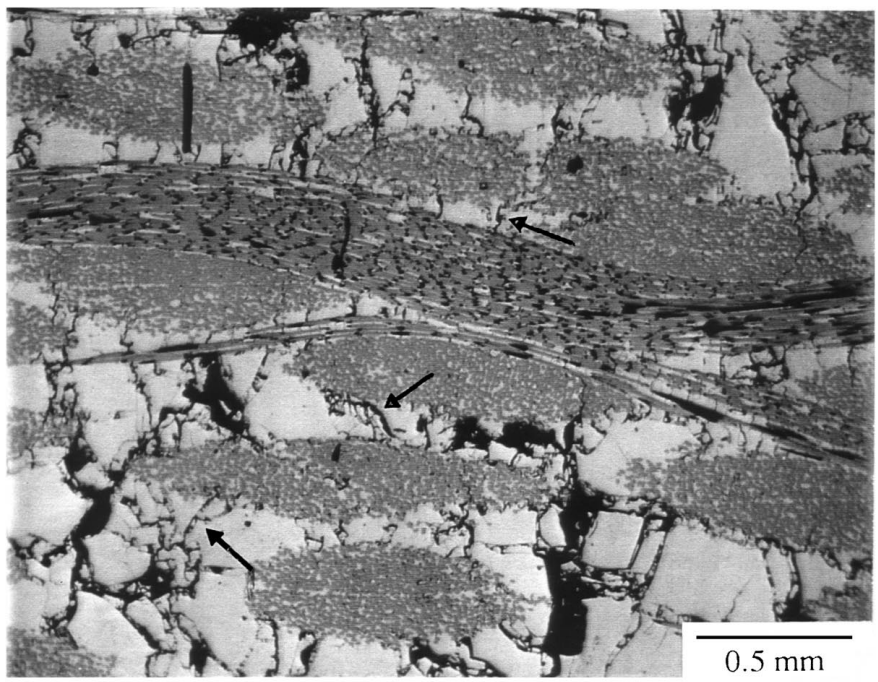

(b)

Figure 13 Optical micrograph of the CMC under various conditions showing the microstructures: (a) P30 sample, (b) P80 sample and (c) PNH_3 sample. (*Continued*).

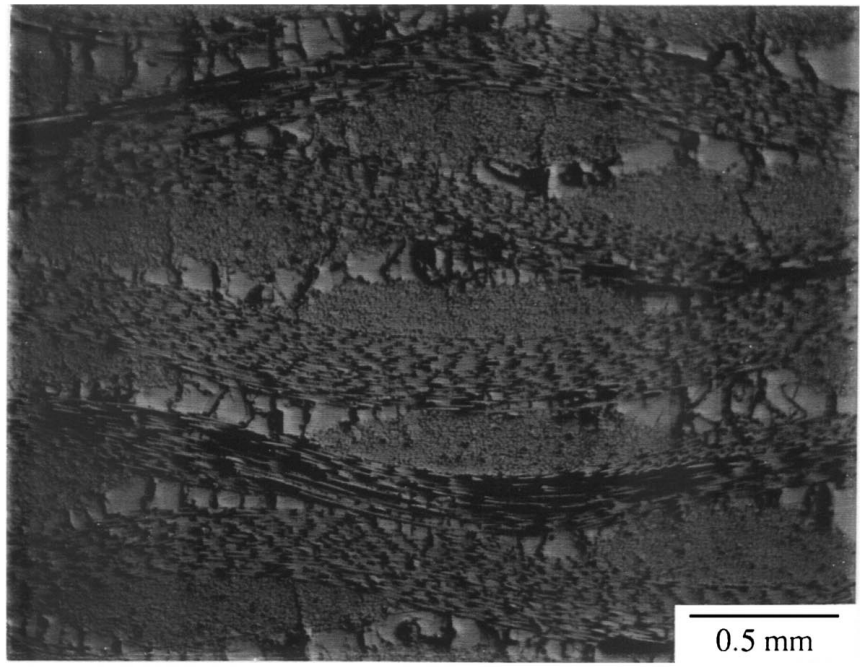

(c)

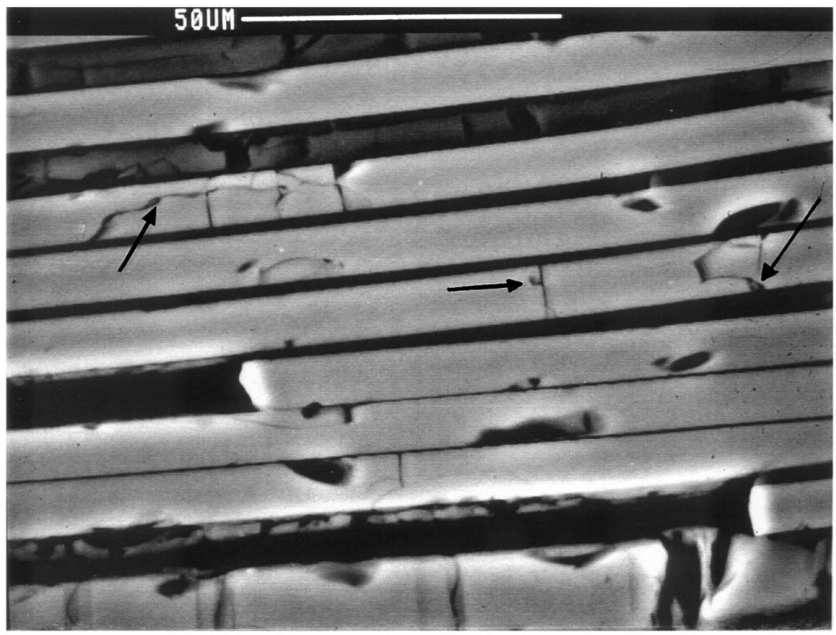

(d)

Figure 13 (*Continued*).

to PNH_3. The pyrolysis in ammonia resulted in the incorporation of 3.9% N in composite with as little as 1.5% C. On the other hand pyrolysis in Ar resulted in approximately 12% C in the composite. It is evident from the Table VI that, the autoclave cure pressure did not affect the chemistry of the final product. P80 had a slightly lower volume fraction of fibers but was slightly richer in carbon when compared to P30.

3.3.3. Development of microstructure

Representative samples were cut from the three panels, polished and mounted for microscopic observations. Fig. 13a–c show low magnification optical micrographs of the cross-section of the panels. The panels were well compacted and the warp and fill fibers are seen. It has been shown that pyrolysis of polysiloxane polymers leads to the formation of micro and nano pores [21]. In all the samples the extent of open porosity is measured while the extent of closed porosity (both nano and microporosity) is unknown. Porosity levels in the composites were $\leq 6\%$.

The large cracks seen in the matrix are indicative of a weak matrix, a consequence of the dissimilar shrinkage of fiber and matrix during pyrolysis and cool down from temperature. These cracks were formed during

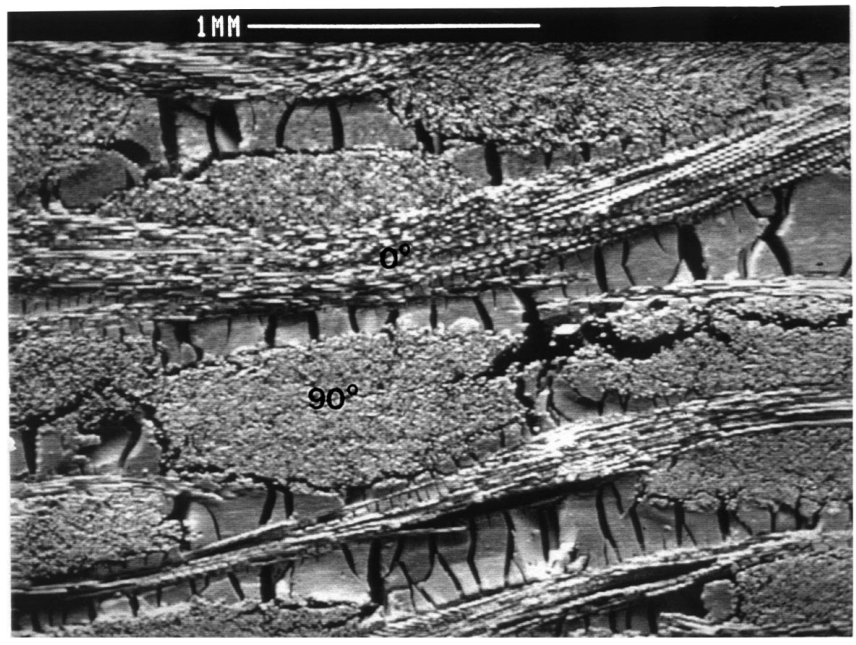

Figure 14 Low magnification SEM micrograph showing the cracked structure after first pyrolysis.

the first pyrolysis cycle (CMC-0) and contribute to the interconnected porosity. This is apparent from Fig. 14, which shows a low magnification SEM picture of a Blackglas matrix composite after the first pyrolysis cycle. The figure shows the network of cracks formed during the first pyrolysis cycle. The cracks were filled up during the subsequent reinfiltration and pyrolysis steps. Examination of the matrix cracks at higher magnification indicate that the material at the edges of the cracks are chemically different compared to the rest of the matrix. Fig. 15a and b are high magnification SEM images along with Si (Fig. 15c) and O (Fig. 15d) energy dispersive X-ray maps of the regions in Fig. 15b. The regions around the crack are richer in oxygen an indication that trapped oxygen and/or trace amounts of oxygen present in the Ar reacted with cured polymer during the cure step and became included in the ceramic in the pyrolysis stage. Pathways for oxygen are retained through the reticulated crack in the subsequent pyrolysis steps. Although cracks are also formed in the fiber rich areas (Fig. 15a), these cracks are filled up and the fibers remain properly spaced and completely wetted by the matrix.

3.3.4. Effect of processing variables

Of the two processing variables studied the autoclave cure pressure did not have a significant effect on the composite microstructure and chemistry. The apparent porosity of the CMCs is not a function of the compaction pressure as shown in Table VI. The rationale behind increasing the cure pressure was to ensure good wetting and compaction. Further it was expected that increasing the pressure would increase fiber volume fraction. The advantages of increasing the pressure were not realized. Curing the panels at 30 psi pressure ensured good wetting and compaction. In fact, higher pressures were detrimental. When higher cure pressures of 80 psi are used, extensive cracking occurs in the fibers in the top and bottom plies as shown in Fig. 13d. This top ply crack cracking is absent in P30 and PNH_3 which were both cured at 30 psi. In addition, the number and size of the cracks in the P80 is larger compared to the P30 as seen in Fig. 13a and b. It is concluded that the higher cure pressure in the former case resulted in matrix cracking resulting in a larger density of cracks in the final product.

On the other hand, pyrolysis in ammonia atmosphere resulted in significant differences in processing steps, matrix chemistry and microstructure of the composites. Pyrolysis resulted in substitution of C with N in the matrix. Of all the composites, the number of cracks is most extensive in PNH_3 (Fig. 13c). Pyrolysis in NH_3 leads to larger shrinkage (more of the C is lost and not much of it compensated by an increase in N) yielding a weak porous matrix. Pyrolysis in NH_3 yields a slightly larger porosity levels.

3.3.5. Oxidation of Blackglas matrix CMCs

Long term stability of the Blackglas matrix CMCs is critical for prolonged use at elevated temperatures. When exposed to elevated temperatures there are two sources of oxidation (i) Burn out of the carbon coating on the Nextel fibers and (ii) Intrinsic oxidation of Blackglas matrix. It was shown by Gonczy *et al.* [19] using thermo gravimetric analysis that C-coating thickness played an important role in determining the total weight loss on heat up from 25 to 900 °C. In their studies it was shown that this weight loss occurred at approximately 650 °C. The weight lost on heating up Nextel 440 fabric coated with different thickness of C-coating is shown in Fig. 15 [19]. Thermogravimetric experiments of the Nextel fabric coated with carbon were performed in a Seiko TGA by heating in the range of 25–1000 °C at 10 °C/min in an environment of flowing air (100 cc/min). Relative weight of the sample as a function of temperature is shown in Fig. 16. The carbon

burn out occurs between 570 and 620 °C with a total weight loss of 2.9 wt %. Comparison of this data with Fig. 15 indicates that the carbon coating thickness on the Nextel 440 fabric is approximately 0.15 μm. Both the 6 and 12 ply CMC panels processed under the three different conditions were oxidized for up to 500 h in a furnace in a static air environment at 1000 °C. The samples were periodically removed, weighed and reintroduced into the furnace. The results of the oxidation tests are presented in Fig. 17.

The oxidation experiments indicate that composites pyrolyzed in an NH_3 environment resulted in only a 1% decrease in weight after as long as 500 h at 1000 °C. The NH_3 pyrolyzed panels have approximately 28 vol % Nextel fibers and the 1% total weight loss corresponds well with the carbon coating burn out. The matrix in the NH_3 pyrolyzed panels is stable as the C and N are bonded to the Si. On prolonged oxidation there is even a small increase in weight which corresponds to the oxidation of the Si in the matrix yielding SiO_2. On the other hand, on oxidation, the Ar pyrolyzed panels exhibit as much as a 5 wt % decrease in weight. Of this 1 wt % is accounted for by carbon coating burn off. The other 4 wt % is due to the oxidation of the pyrolytic (graphitic) carbon present in the matrix. The presence of the graphitic carbon is verified by the XPS

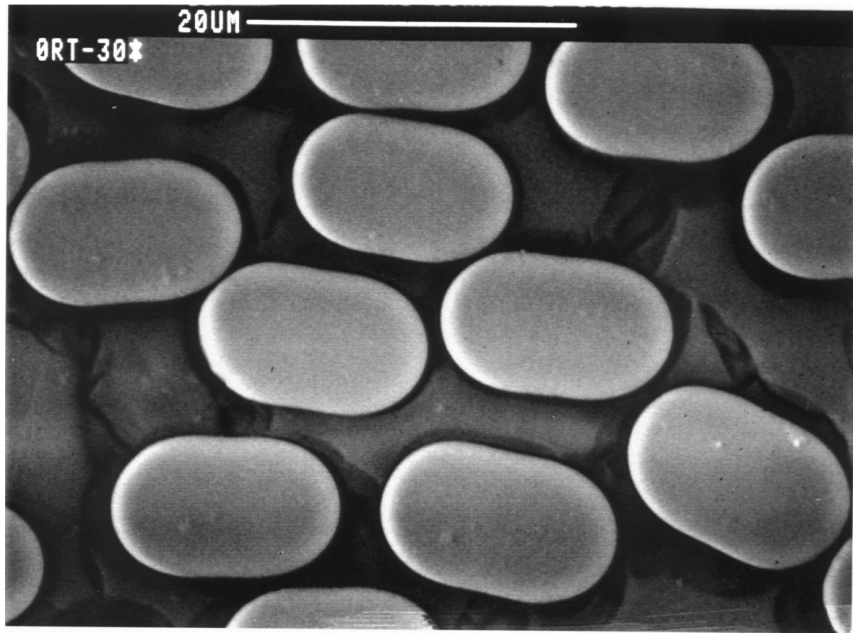

(a)

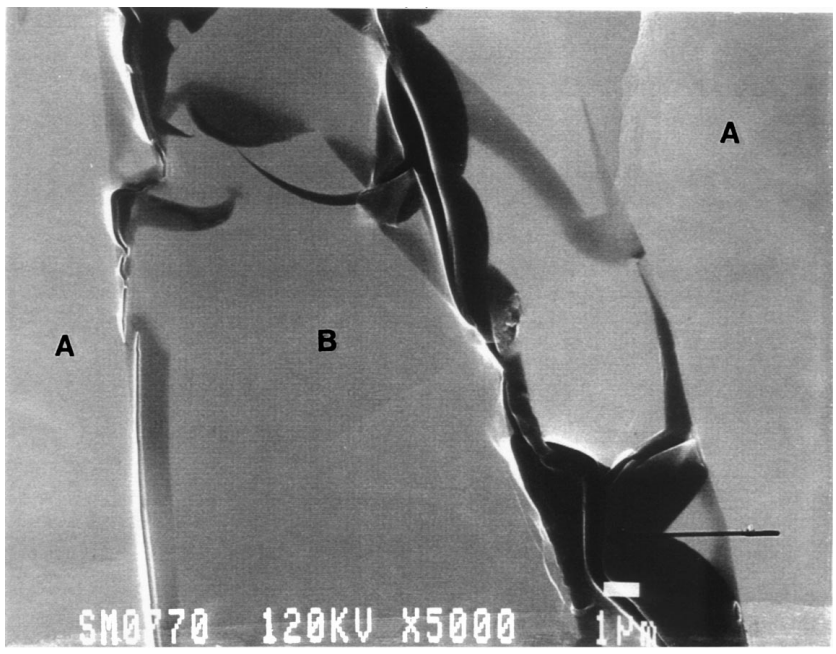

(b)

Figure 15 Scanning electron micrograph of the P80 sample showing the presence of cracks in the matrix in (a) fiber rich areas, (b) matrix rich regions together with the (c) silicon and (d) oxygen X-ray dot map for the region. Dot map clearly shows that darker areas in (b) are richer in oxygen. Regions A are the matrix from first pyrolysis, while regions B are reinfiltrated matrix. (*Continued*).

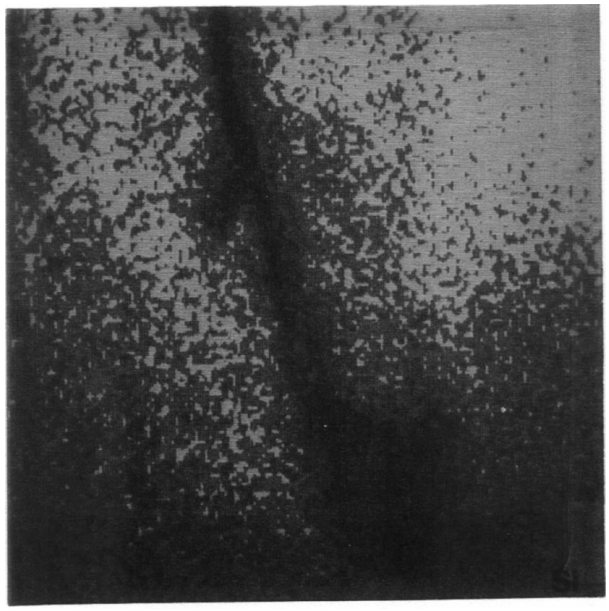

(c)

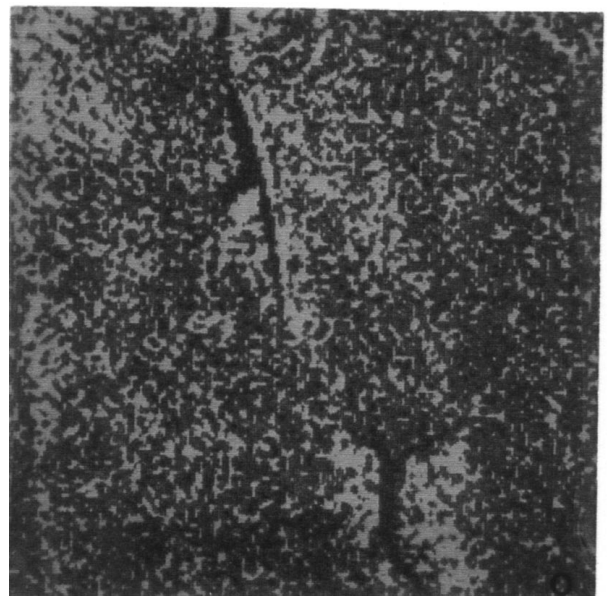

(d)

Figure 15 (*Continued*).

data in Fig. 10. These results indicate that the Ar pyrolyzed panels are less oxidation resistant than the NH_3 pyrolyzed panels.

3.3.6. Thermomechanical analysis of Blackglas matrix CMCs

Thermomechanical analysis was performed from 25 to 1000 °C on all the Blackglas matrix composite panels in both the in-plane and out-of-plane orientations and the data is summarized in Table VII. In the in-plane orientation $\alpha_{PNH_3} > \alpha_{P30} > \alpha_{P80}$ while in the out-of-plane orientation $\alpha_{PNH_3} < \alpha_{P30} < \alpha_{P80}$. The density of the composites follow the trend $\rho_{PNH_3} < \rho_{P30} < \rho_{P80}$ and the porosity content in the composite is in the order of $V_{PNH_3} > V_{P30} \approx V_{P80}$ (see Fig. 12). In addition the density of matrix cracks is the largest in the NH_3 pyrolyzed samples. The CTE of the fibers are the same in all the cases and all three composites have very similar volume fraction of fibers (28–31 vol %). Hence, the largest in-plane CTE in PNH_3 may be attributed to the presence of a large number of matrix cracks (see Fig. 15) which result in a lower constraint for the expansion of the Nextel fibers. The resulting composite CTE is similar to the CTE of the un-reinforced Nextel 440 fabric. The out-of-plane CTE is controlled primarily by the expansion of the matrix. The larger porosity content in the matrix of the PNH_3 results in easy accommodation of the expansion of the panel resulting in a lower overall CTE in the out-of-plane orientation. Although the porosity levels of P30 are almost the same as that of P80, α_{30} is less than that of α_{80}. This is probably due to slightly lower volume fraction and to fiber damage in P80, which reduces the composite CTE.

TABLE VII Coefficient of thermal expansion of Blackglas matrix composites reinforced with Nextel™ 440 in the temperature range of 200–750 °C

Panel ID	Sample orientation	CTE[a] PPM/°C (200–750 °C)
Nextel™ 440 Fabric[20]	—	5.4 in the 25–1000 °C range
P30	In-plane	4.7
	Out-of-plane	3.7
P80	In-plane	4.4
	Out-of-plane	4.1
PNH_3	In-plane	5.5
	Out-of-plane	3.3

[a]CTE: Coefficient of thermal expansion.

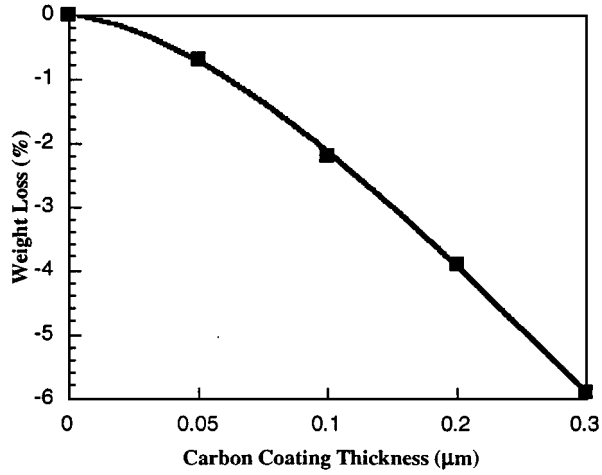

Figure 16 Weight lost on heat up of Nextel 440 fabric coated with different thickness of carbon coating. The experiment was performed in a TGA in the temperature range of 25–900 °C [19].

3.3.7. Dielectric properties of Blackglas matrix CMCs

Dielectric properties of representative specimens from each of the three processing conditions were evaluated using the waveguide technique at a frequency of 10 GHz. In addition specimens oxidized for up to 100 h

TABLE VIII Dielectric properties at 10 GHz of Blackglas matrix composites reinforced with Nextel 440 fabric under various processing conditions and oxidation states

Oxidation condition[a]	Nextel 440 (Uncoated) K'^{20}	Nextel 440 (Uncoated) K''^{20}	P30 K'	P30 K''	P80 K'	P80 K''	PNH_3 K'	PNH_3 K''
As-Processed	5.7 @ 9.375 Ghz	0.015 @ 9.375 GHz	11.0	> 1.0	28.0	> 1.0	3.9	> 1.0
5 h	—	—	4.3	0.22	4.3	0.22	4.0	0.22
10 h	—	—	4.3	0.22	4.3	0.22	4.0	0.11
50 h	—	—	4.3	0.22	4.3	0.22	4.0	0.13
100 h	—	—	4.3	0.22	4.3	0.22	4.0	0.13

[a]P30 and P80 were oxidized at 982 °C while PNH_3 was oxidized at 816 °C.

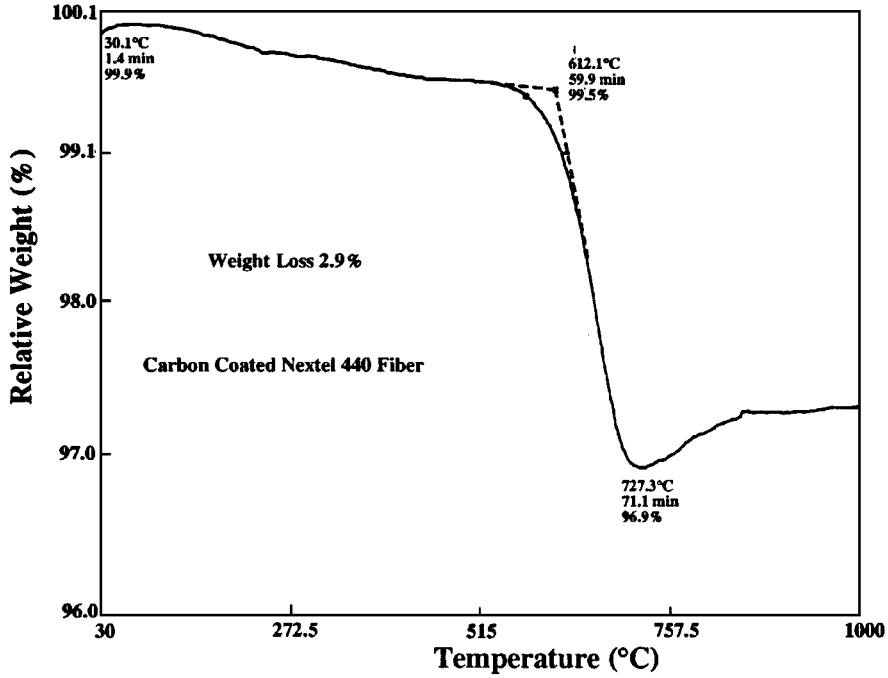

Figure 17 Thermogravimetric analyzer plot of relative weight (as a percentage of original weight) as a function of temperature of the C-coated Nextel 440 fabric on heat up from 25–1100 °C at 10 °C/min in an environment of flowing air.

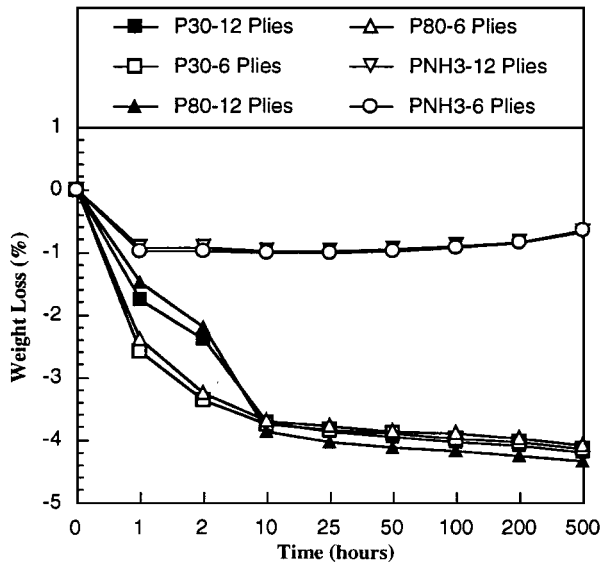

Figure 18 Weight loss as a function of oxidation time of Blackglas matrix CMC's at 1000 °C in a static air environment in a furnace. Three processing conditions were studied (i.e. P30, P80 and PNH_3) and two panel thicknesses of 6 and 12 plies were examined.

at 1000 °C were examined and results are summarized in Table VIII. In the as-processed state the dielectric constant K' in the Ar pyrolyzed sample is in the range of 11–28 whereas in the NH_3 pyrolyzed sample it is approximately 4.0. The difference in dielectric constants in the two processing conditions arise due to the difference in the matrix chemistry. The Ar pyrolyzed panels have as much as 8 wt% graphitic carbon (see Fig. 10) which makes them very electrically conductive resulting in a large value of K'. On the other hand the NH_3 pyrolyzed panels have network C and N bonded to Si in the matrix resulting in lower electrical conductivity and lower dielectric constant. Both categories of samples have a dielectric loss factor K'' of ≈ 1.0. On oxidation for as little as 5 h at 982 °C for the Ar pyrolyzed samples resulted in a significant drop in K' to 4.3 and this value of K' remains stable even after 100 h of oxidation. This drop in K' can be attributed to a burn off of the graphitic carbon present in the matrix. The K' in the NH_3 pyrolyzed sample remains stable around 4.0 as there is little change on the chemistry of the matrix on prolonged oxidation at 816 °C.

4. Conclusions

The following generalized conclusions can be drawn:

1. The curing behavior of Blackglas precursor solution is strongly dependent on the catalyst content. The curing is an extremely fast process.

2. Ceramic structure and ceramic yield of Blackglas is not dependent on the curing conditions. The ceramic contains free and network carbon and yields are ~ 82%.

3. Processing of CMCs leads to shrinkage cracking and porosity. Autoclave cure pressure did not significantly affect the chemistry and porosity in the CMC. However the cure pressure increases cracking and damage in the P80 CMC.

4. Processing in ammonia increases the cracking and porosity in the CMC. Also ammonia pyrolysis introduces N in the PNH_3 composite.

5. Crack like interfaces are present in the fully densified CMCs. These interfaces significantly deteriorate the oxidation resistence.

Acknowledgements

Support provided by the Mechanical and Aerospace Engineering Department and the Materials Science and Engineering Program at University of Texas @ Arlington is gratefully acknowledged. This work was supported in part by an IRAD project at Northrup Grumman Corporation, Dallas, TX, Mr. Donald Box, Program Manager. Materials were provided by Allied Signal Corporation, Des Plaines, IL. The authors wish to thank Dr. Steve Gonczy and Dr. Roger Leung for useful discussions.

References

1. S. YAJIMA, Y. HASEGAWA, J. HAYASHI and M. IIMURA, *J. Mater. Sci.* **13** (1978) 2569.
2. Y. HASEGAWA, M. IIMURA and S. YAJIMA, *ibid.* **15** (1980) 720.
3. R. M. LAINE and F. BABONNEAU, *Chem. Mater*. **5** (1993) 260.
4. W. R. SCHMIDT, V. SUKUMAR, W. J. HURLEY, JR., R. GARCIA, R. H. DOREMUS, L. V. INTERRANTE and G. M. RENDLUND, *J. Amer. Ceram. Soc*. **70** (8) (1990) 2412.
5. R. Y. LEUNG, T. STANFORD and S.T. GONCZY, U.S. Patent 5,258,084, Nov. 2, 1993.
6. L. BOIS, J. MAQUET, F. BABONNEAU, H. MUTIN, D. BAHLOUL, *Chem Mater*. **6** (1994) 796.
7. D. MOCAER, R. PAILLER, R. NASLAIN, C. RICHARD, J. P. PILLOT, J. DUNOGUES, C. GERARDIN and F. TAULELLE, *J. Mater. Sci*. **28** (1993) 2615–2631.
8. F. I. HURWITZ, L. HYATT, J. GORECKI and L. D'AMORE, *Ceram. Engg. Sci. Proc*. **11** (7 8) (1990) 732–743.
9. F. I. HURWITZ, J. Z. GYEKENYESI, P. J. CONROY and A. L. RIVERA, *ibid*. **11** (7 8) (1990) 931–946.
10. S. H. YU, R. E. RIMAN, S. C. DANFORTH and R. Y. LEUNG, *J. Amer. Ceram. Soc*. **78** (7) (1995) 1818.
11. F. I. HURWITZ, Approaches to polymer derived CMC matrices, in Twenty Fourth Inter. SAMPE Technical Conference, Oct 20–22, T950, (1992).
12. B. BOURY, J. P. CORRIU and W. E. DOUGLAS, *Chem. Mater*. **3** (1991) 487.
13. W. R. SCHMIDT, P. K. MARCHETTI, L. V. INTERRANTE, W. J. HURLEY, R. H. LEWIS, R. H. DOREMUS and G. E. MACIEL, *ibid*. **4** (1992) 937–47.
14. ASTM C 20 -92, Standard test methods for apparent porosity, apparent specific gravity, and bulk density of burned refractory brick and shapes by boiling water, Annual Book of ASTM Standards, Vol. 15.01 (1994).
15. E. L. LUKEVITS and M. G. VORONKOV, Organic Insertion Reactions of Group IV Elements, Consultants Bureau, NY, USA (1966).
16. W. NOLL, "Chemie und Technologie der Silicone" (Verlag Chemie, Weinheim, Germany, 1968).
17. D. WEWERS, "Silicones, Chemistry and Technology" (CRC Press, Boca Raton, FL, USA 1991).
18. D. R. ANDERSON, in Chemical Analysis Vol. 41, "Analysis of Silicones," edited by A. Lee Smith (John Wiley & Sons, NY, 247, 1975).
19. S. T. GONCZY, R. Y. LEUNG and J. EVANS, "Oxidation Effects on Fibrous Fracture in Blackglas™ Composites Reinforced with 3-D and 2-D Nextel™ 440 (Carbon-Coated)", Presented at 16th Annual Conference on Composites, Materials and Structures, 15th Jan. 1992., Cocoa Beach, FL.
20. "Properties of Nextel™ 312 and 440 Ceramic Fibers", Ceramics Materials Dept. Bulletin, 3M Corporation, St. Paul MN 55144, Jan. 1993.

Received 22 July
and accepted 28 September 1998